Concentration profile distortion under ion beam mixing: An example of Levy flight

D. Simeone[1,*] and L. Luneville[2,†]
[1]*CEA, DEN, SRMA, LA2M, Equipe Mixte MFE, F-91191 Gif sur Yvette, France*
[2]*CEA, DEN, SERMA, LLPR, Equipe Mixte MFE, F-91191 Gif sur Yvette, France*
(Received 4 November 2009; published 9 February 2010)

In order to model the evolution of concentration profiles induced by ion beam mixing in thick layers, Monte Carlo simulations were performed to study in detail the transition probability controlling the evolution of this profile within the binary collision approximation. We demonstrate that this transition probability can be factorized in two distinct functions. The first one can be understood as a scale factor. The second one controls the dynamics of ion beam mixing which can be analyzed as a Levy flight. The power law form of the tail of this function closely linked to the cross section of a collision event is responsible for long tails of concentration profiles. We demonstrate that the Levy flight nature of ion beam mixing induces an enhancement of the evolution of the initial concentration profile.

DOI: 10.1103/PhysRevE.81.021115 PACS number(s): 05.40.Fb, 05.60.Cd, 81.40.Wx

I. INTRODUCTION

Ion solid interaction is of significant interest to both academic and industrial researchers [1,2]. In particular, ion solid interaction is relevant to many applications in corrosion resistance, adhesion, and structural stability of materials under irradiation [1]. Ion implantation revolutionized the microelectronic industry offering a control over the number and depth of dopant atoms in semiconductor materials [3,4]. Nowadays, the development of high current and high voltage implanter allows not only to deposit a small amount of impurity atoms but also to tailor buried new compound layers using high fluence implantations [4]. The migration of atoms occurring during the ion beam mixing is of paramount importance to investigate phase stability and new properties of these compounds [5]. The molecular dynamics (MD) method has been extensively used to describe the diffusion of atoms in displacement spikes forming the displacement cascades [5,6]. However, MD simulations of a displacement cascade initiated by high energy particles (above a few tens of keV) is very time consuming and is out of reach [5]. The binary collision approximation thus remains a useful theoretical framework to study the ion beam mixing created by implantation [3,4]. Many models first developed in the 1980s by Sigmund and Gras Marti defined the so called "relocation cross section" to quantify the diffusion of atoms far from their initial positions [7,8]. Many experimental works point out that atoms involved in a cascade display a Gaussian displacement distribution at low temperature, where defect mediated diffusion is negligible [3,4,9]. However, experimental profiles produced by irradiation of thick targets by high energy particle, i.e., few thousands of keV, exhibit unexpectedly long tails [4,10,11]. A question then arises: what is the physical mechanism responsible for this unusual diffusion under ion beam mixing?

Whereas the "relocation cross section" formalism can be used to estimate ion beam mixing in thin layers [7,8], no quantitative determination of ion beam mixing in thick layers have been yet performed to the authors' knowledge. This effect remains one main limitation in synthesizing nanocomposites with a well defined compositional patterning using ion beams [12,13]. The challenge for exploiting this potential lies in controlling at a nanometric scale this atomic mixing. The ion beam mixing in thick layers constitutes a general problem of relevance in nuclear waste storage [14], metastability of solids under irradiation [1,2] and material processing [3,4].

In this work, we quantify this effect by identifying physical key parameters. As collision events are statistically independent, a succession of collisions can be considered as a Markov process. We then describe the ion beam mixing as a continuous random walk process in the first part of this work. Using realistic cross sections to model atomic collisions [15], Monte Carlo (MC) simulations were performed to study in detail the transition probability, $p(x,\Delta x)$, associated with this random walk process. Results of MC simulations clearly show that this transition probability exhibits a power law tail. In the second part of this work, we demonstrate that this transition probability exhibits peculiar properties closely linked to the properties of cross sections describing collision events. From the power law form of the tail of $p(x,\Delta x)$, rare collision events dominate the dynamic of ion beam mixing. Finally, we study in detail this dynamic and show that it can be considered as a Levy flight leading to an enhanced diffusion of particles.

II. MONTE CARLO SIMULATIONS OF THE TRANSITION PROBABILITY

The effect of energetic ions upon solids is associated with various phenomena. Impinging ions deposit energy in the material via collisions with the atoms and the electrons in the solid [16,17]. This energy deposition leads to sputtering and radiation damage in the medium [18]. In addition to these effects, atoms set in motion by incident particles can travel over large distances leading to atomic mixing [3,4]. This athermal transport of atoms only occurs in the irradiated area and approximately over the range of the incident ion in the

*david.simeone@cea.fr
†laurence.luneville@cea.fr

solid. During ion bombardment, collisions with electrons and atoms at rest are responsible for this athermal transport of matter [3,4,7,8]. The slowing down of atoms in motion by the electrons can be understood as a viscous friction force [17]. It does not lead to direct displacement of atoms in metallic targets. This point explains why the electronic slowing down has been neglected in this work. Moreover, even if collisions occurring during the slowing down of atoms set in motion are a sum of single events, the amount of such collisions is so large that continuous functions can accurately describe the ion beam mixing over several hundreds of nanometers [8].

Within the "relocation cross section" theory framework [7,8] usually used to describe the ion beam mixing, the central assumption is the stationarity of the cross section describing collision events in thin layers. In other words, the energy loss of the incident beam needs to be small in thin layers. In infinite or thick targets, incident particles stop in the medium. So, such an assumption on the stationarity of the cross section does not hold. The relocation cross section $\frac{d\sigma(x,\Delta x)}{d\Delta x}$ introduced previously by Sigmund *et al.* [7] is the ratio of $p(x,\Delta x)$ by $\mathcal{N}$ the number of atoms in the target. The function $p(x,\Delta x)$ quantifies the ability of an atom at depth x to be displaced of Δx during the irradiation. Introducing $c(x,t)$ the concentration of displaced atoms at the position x in the layer at the time t, the amount $\mathcal{N}c(x,t)p(x,\Delta x)d\Delta x$ is the number of atoms initially at rest at the position x relocated to the layer $(x+\Delta x)$ under irradiation at the time t. In order to study in detail this transition probability $p(x,\Delta x)$ in infinite targets, the set of trajectories of atoms set in motion has been calculated from MC simulations. To obtain a clear and simple description of this function $p(x,\Delta x)$, we only consider the ion beam mixing induced by the bombardment of a mono atomic target by self ions. Such a simplification allows to maximize the energy transferred to atoms at rest in the solid as well as to clearly define the effective charges of particles in motion in the medium. Moreover, in all our simulations, we neglect the slowing down of particles by the electronic stopping power.

To perform realistic MC simulations, we sample the energy transferred to an atom at rest during a collision. An incident particle with energy E looses an amount of energy T during a single collision event according to the probability density $k(E,T)$ [19]. This function $k(E,T)$, depends only on the kinetic energies of the incident particle E and T before and after the collision. This function is equal to $\frac{d\sigma(E,T)}{dT}\frac{1}{\sigma(E)}$ where $d\sigma(E,T)$ and $\sigma(E)$ are the differential and total cross sections. The BZL differential cross section derived from the universal Biersack Ziegler Littmark interatomic potential [15,20] is used in this work to define accurately the energy transferred to recoils over a large energy range [20,21]. For a given energy E, the efficiency of this cross section depends only on the average ionic charge [20], Z, between incident particles and atoms at rest in the solid. As no analytical formulation for the BZL differential cross section is available, the rejection method [22] is used in our MC simulations to sample the random variable T. The MC simulation stops when the kinetic energy of the knocked atoms initially at rest is equal to E_d, the threshold displacement energy.

We also need to define the distribution of the length l traveled by a particle after a single collision event. We assume that memory effects from a collision to the next due to spatial correlation between scattering atoms can be neglected in our simulations. This assumption is largely used in the calculation of penetration ranges of energetic ions in solids [15,20]. As clearly shown in Appendix A, the probability density function to obtain l for a given T energy value then follows an exponential law [23,24],

$$p_C(l|T) = \mathcal{N}\sigma(T)e^{-\mathcal{N}\sigma(T)l} = \frac{1}{L(T)}e^{-l/L(T)}, \tag{1}$$

where $L(T)=\frac{1}{\mathcal{N}\sigma(T)}$.

As this exponential law does not exhibit a narrow tail, the distribution of lengths derived from Eq. (1) cannot be reduced to its mean-free path $L(T)$. However, this mean-free path is extensively used in the "relocation cross section" theory [7] to define the length traveled by recoil atoms in a displacement cascade. In our simulations, the length l traveled by a particle between two successive collisions is sampled using the inversion method from Eq. (1).

This sampling, both in energy and in length then allows to determine accurately the trajectory of each displaced atom. In all our MC simulations, $\mathcal{N}$, and E_d were equal to 1 Å^{-3} and 10 eV, respectively. MC simulations were performed with a charge Z equal to 1, 2, 5, 10, 20, 40, 45, 60, and 90 to investigate the efficiency of the interatomic potentials on the relocation of atoms under ion beam mixing.

From MC simulations, we extracted the joint probability $p(x,\Delta x)$. This function quantifies the distribution of atoms initially at rest at the position x relocated after many collisions by the distance Δx along the direction of the incident beam. All our simulations performed with different projectiles and energies have always shown that this joint probability can be factorized in two distinct functions $g(x)$ and $p(\Delta x)=\int p(x,\Delta x)dx$. Our simulations establish that this factorization of $p(x,\Delta x)$ does not depend on the peculiar shape of the cross section. This result extends previous analytical works performed to study the ion beam mixing in thin layers and power law cross sections [8] to thick layers and more realistic BZL cross sections [8,21]. Introducing $L=L(E_0)$ associated with the energy E_0 of the incident beam, different insets on Fig. 1 display the comparison between $g(x)$ and $\frac{F_D(x)}{E_0}$ as a function of $\frac{x}{L}$ for different Z values where $F_D(x)$ is the deposited energy by all atoms set in motion [4,25]. Moreover $g(x)$ exhibits significant variations for $\frac{x}{L}$ values ranging from 1 to 100.

Figure 1 displays also the evolution of $p(\Delta x)$ as a function of $\frac{\Delta x}{L}$ for different Z values. The function $p(\Delta x)$ exhibits significant variations for $\frac{\Delta x}{L}$ values ranging from 0.01 to 1. From the analysis of Fig. 1, it clearly appears that significant variations of $g(x)$ and $p(\Delta x)$ occur over different length scales. Moreover, the tail of $p(\Delta x)$ has a power law form as a function of $\frac{\Delta x}{L}$ over 2 decades. This power law form for the tail of $p(\Delta x)$ indicates the absence of a characteristic size of jumps and is responsible for the Levy flight nature of particle trajectories [26,27]. The analysis of numerous MC simulations performed with Z values ranging from 1 to 99 have clearly shown that the exponent of this power law depends only on Z, i.e., the efficiency of the interaction associated

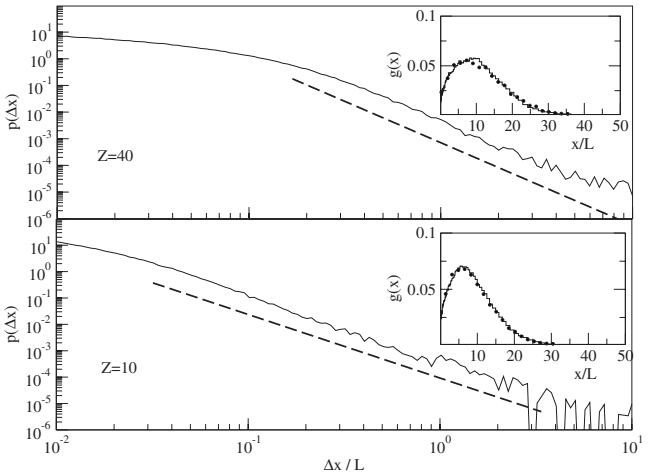

FIG. 1. Variation in $p(\Delta x)$ (full line) extracted from MC simulations as a function of $\frac{\Delta x}{L}$ for different Z values (top $Z=40$; Bottom $Z=10$) at a given energy $E_0=10^6$ eV. The different $p(\Delta x)$ functions display significant variations for Δx values ranging from $10^{-1}L$ to $10L$. Moreover, these curves exhibit a power law tail $(\frac{\Delta x}{L})^{-(1+q_c)}$ at least over two decades (dashed lines). The insets display the comparison between $g(x)$ (line) and $\frac{F_D(x)}{E_0}$ (dots). These insets clearly show an excellent agreement between these functions over a large x range.

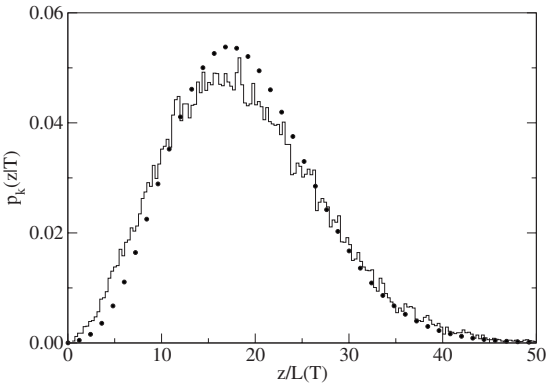

FIG. 2. Comparison between $p_k(z|T)$ (line) extracted from MC simulations and the Gamma distribution $\Gamma[z;1+q_c,L(T)]$ (dots) for $Z=10$, $T=10^5$ eV and $k=60$. This graph displays a good agreement between these two functions over a large $\frac{z}{L}$ range.

with a collision event, written as $q_c(Z)$. The variable q_c is the dimension of the point set visited by the Levy flight [28], as demonstrated in Appendix C and in agreement with previous works on Levy flights [27]. As $p(\Delta x)$ is associated with the jumps of displaced atoms in the displacement cascade, this function then captures all the underlying physics of elementary collision events responsible for the ion beam mixing. We will now discuss the origin of the peculiar form of $p(x,\Delta x)$ giving rise to the Levy flight.

III. THEORETICAL CALCULATION OF $p(x,\Delta x)$

By analogy with the multiple scattering theory, we follow a probabilistic approach of collisions events [23,24] to calculate $p(x,\Delta x)$. Within this framework, no assumption on the straggling of particles is needed. This work then extends previous works on ion beam mixing based on the continuous slowing down approximation where the straggling is always neglected [7,8]. To understand the physical mechanism responsible for the factorization of $p(x,\Delta x)$ and the unusual power law form of $p(\Delta x)$, we need to describe accurately the trajectory set of particles in motion in a medium at a position x.

For one collision event, the probability density associated with the random variable T describing the energy of the particle after a collision is $K_1(E,T)=k(E,E-T)$. As two collisions are statistically independent, the probability density function to obtain the energy T after two collisions is then $K_2(E,T)=\int_T^E K_1(E,U)K_1(U,T)dU$. The calculation of $K_n(E,T)$ after n collision events is straightforward. We then determine the length traveled by a particle of energy T along its trajectory. As collision events are statistically mutually independent, the distribution of the length traveled by this particle is reduced to

$$p(l|T)=\int_{E_d}^{T}\sum_{n=0}^{\infty}K_n(T,U)p_C(l|U)dU=\int_{E_d}^{T}h(T,U)p_C(l|U)dU. \tag{2}$$

Where $p_C(l|U)$ is the density probability associated with a flight of a particle with a kinetic energy U between two collisions as calculated according to Eq. (1), the function $h(T,U)\sim U^{-1}$ is the energy loss of a particle with energy T until it stops [21,28].

From Eq. (2), $p(l|T)$ can be analytically calculated and can be approximated by $\frac{1}{l}exp^{-l/L(T)}$ over a large $\frac{l}{L(T)}$ range (Appendix B). By analogy with the theory of multiple scattering [23,29], the total length z traveled by a particle set in motion with the energy T until it stops in the matrix is equal to $z=\Sigma_{j=0}^{N(T)}l_j(T)$ where $N(T)$ is the random variable associated with the number of collisions occurring along the trajectory of the particle. Along a trajectory, $p(z|T)$ is obtained by summing over all mutually exclusive collisions events [19]. This probability is then equal to $\Sigma_{k=0}^{+\infty}p(N(T)=k)p_k(z|T)$ where $p_k(z|T)$ is the k-fold convolution product of $p(l|T)$.

Within the "relocation cross section" theory framework, $N(T)$ is always supposed small to agree with the assumption of the stationarity of the cross section describing collision events [7]. The probability density of $N(T)$ then reduces to a Poisson law. In thick and infinite layers, $N(T)$ is always large and its probability density differs from a Poisson distribution as observed in our MC simulations (but not shown here). For large k values, the Large Deviation theorem (Appendix D) is an elegant tool to approximate $p_k(z|T)$. Figure 2 displays the comparison between $p_k(z|T)$ extracted from our MC simulations and derived from the application of the Large Deviation theorem. The function $p_k(z|T)$ can be fairly well approximated by a Gamma distribution, $\Gamma[z;1+q_c,L(T)]$, independent of k over a large $\frac{z}{L}$ range. Replacing $p_k(z|T)$ by this approximate expression, $p(z|T)$ becomes independent of k and behaves like $p_k(z|T)$. This point highlights the main interest of the Large Deviation theorem. As the asymptotic

expansion of $p_k(z|T)$ is, by definition, independent of k, the distribution of the number of collisions is now irrelevant and can be omitted in the calculation of $p(z|T)$. From this analysis, our model is then able to quantify the effect of ion beam mixing whatever the thickness of the layer is. No assumption on the distribution of $N(T)$ is needed whereas the Poissonian nature of $N(T)$ is required in the relocation cross section formalism [7]. The scale parameter of the gamma distribution describing $p(z|T)$ is equal to $L(T)$ the mean-free path of $p_C(l|T)$ as pointed out in previous works [7] and its shape parameter, $1+q_c$, is associated with the dimension of the trajectories set [28] as demonstrated in Appendix C.

In the last step of our analysis, we need to link z with the projected length Δx along the direction of the incident beam. We introduce the deviation angle ψ between the trajectory of the particles of energy T set in motion by particles of energy E at the position x and in the direction of the incident beam in the laboratory frame. The projected jump along this direction Δx is then equal to $z\cos(\psi)$. As this deviation occurs during a single collision event, the probability density function associated with the random variable T is equal to $k(E,T)$. As this function exhibits large values only in the neighborhood of E_d, small deviations mainly occur. This point implies that $\psi \sim \pm\sqrt{\frac{T}{E}}$. Moreover, $\cos(\psi)$ can be replaced by its average value $\langle\cos(\psi)\rangle = \int_{E_d}^{E}\cos(\psi)k(E,T)dT \sim [1-\int_{E_d}^{E}\frac{T}{E}k(E,T)dT])$. By definition of the stopping power, $\langle cos(\psi)\rangle$ then reduces to $(1-\frac{S(E)}{2E\sigma(E)})$.

Under such an assumption, Δx becomes proportional to z and can never be negative. Negative values of Δx are thus associated with large deviations of the angle ψ which have been neglected in our analysis [23]. From the scaling properties of the Gamma function, Δx follows a Gamma distribution with the same shape parameter than z but with a scale parameter reduced to $\hat{L}(T)=L(T)/(1-\frac{S(E)}{2\sigma(E)E})$. The joint probability $p(x,\Delta x)$ is then obtained weighting $p(\Delta x|T)$ over all trajectories of particles at the position x in the target according to

$$p(x,\Delta x) = \frac{F_D(x)}{E_0}\int_{E_d}^{E_0}\Gamma[\Delta x;1+q_c,\hat{L}(T)]\frac{E_d}{T^2}dT, \qquad (3)$$

where $\frac{E_d}{T^2}$ is the fraction of atoms with energy T set in motion by particles with energy E_0 [7,18,28].

Equation (3) establishes the factorization of $p(x,\Delta x)$ in two distinct functions in agreement with results of MC simulations plotted on Fig. 1. From Eq. (3), $p(\Delta x)$ then reduces to $(\frac{\Delta x}{L})^{-(1+q_c)}$ for large $\frac{\Delta x}{L}$ values (Appendix E) in agreement with results of MC simulations plotted on Fig. 1. This point assesses the validity of Eq. (3) and justifies the assumption linking z to Δx.

This analysis demonstrates that the factorization and the power law form of the tail of $p(x,\Delta x)$ are due to the particular form of the BZL cross section which describes a single collision event. We will discuss the impact of this unusual shape of $p(x,\Delta x)$ on the evolution of a concentration profile.

IV. LEVY FLIGHT AND ENHANCED DIFFUSION

Considering a semi-infinite target with a planar surface at $x=0$ and an initial concentration profile $c_0(x)$, we now consider the evolution of this profile under irradiation. Neglecting sputtering effects which erodes the surface layer from few Angstroms [8], the evolution of this profile over many nanometers, $c(x,t)$ satisfies the following balance equation:

$$\frac{\partial c(x,t)}{\partial t} = \frac{\phi}{\mathcal{N}}\int_0^{+\infty}[p(x-\Delta x,\Delta x)c(x-\Delta x,t) - p(x,\Delta x)c(x,t)]d\Delta x,$$

$$c(x,0) = \delta(x-0), \qquad (4)$$

where ϕ is the flux of incident particles (particles per unit area and per unit time).

The solution of Eq. (4) is the Green's function of this one-dimensional ion beam mixing problem. By analogy with the random walk [26,27], the function $p(x,\Delta x)$ in the right side of Eq. (4) captures all the underlying physics associated with collision events responsible for the ion beam mixing.

Equation (4) is linear with the flux and describes the modification of an initial concentration profile. The limitation of the validity of Eq. (4) is due to the overlapping of displacement cascades. If the flux is intense, displacement cascades overlap and Eq. (4) is no more linear with the flux. As the occurrence of a collision cascade is a rare event, the probability density function associated with the cascades overlapping follows a Poissonian law [19]. From this analysis, displacement cascades do not overlap as long as the condition $t\frac{\phi p}{\mathcal{N}}<1$ is fulfilled. This condition insures then the validity of Eq. (4). To study in detail this condition, we calculate explicitly $p(x,\Delta x)$. For $\Delta x \sim L$, $p(\Delta x)$ reduces to $\frac{1}{L}$ and $\frac{F_D(x)}{E_0}$ is of the order of magnitude of unity. To avoid the overlapping of displacement cascades, $t\phi$ must be inferior to $\mathcal{N}L$. This condition is fulfilled if $\sigma(E_0)\phi t<1$ where $\sigma(E_0)$ is the total cross section associated with a collision event between an incident particle and an atom in the medium. This condition links a global phenomenon, the evolution of a concentration profile, to the underlying physics responsible for this evolution, a single collision event. For usual fluxes ($\phi \sim 10^{11}$ cm^{-2} s^{-1}) and typical L values of few nanometers (L is equal to 2 nm for $E_0=10^6$ and $Z=10$), the validity of Eq. (4) leads to an irradiation time, $t<10^5 L \sim 10^6$ s. This condition is always fulfilled in implanters and nuclear power plants. Equation (4) then describes accurately the evolution of a concentration profile in a medium under ion irradiation.

The factorization of the transition probability $p(x,\Delta x)$ insures that $\frac{F_D(x)}{E_0}$ acts only as a scaling parameter in Eq. (4). As the variations of $F_D(x)$ and $p(\Delta x)$ occur over different length scales as clearly shown on Fig. 1, $F_D(x-\Delta x)$ then reduces to $F_D(x)$ in Eq. (4) for significant variations of $p(\Delta x)$. The first term in right side of Eq. (4) then reduces to a convolution product. Introducing the reduced variable $w=t\frac{\phi F_D(x)}{\mathcal{N}E_0}$, and the function $\tilde{c}(x,w)=c(x,w\frac{\mathcal{N}E_0}{\phi F_D(x)})$, Eq. (4) becomes

$$\frac{\partial\tilde{c}(x,w)}{\partial w} + \tilde{c}(x,w) = \int_0^{+\infty} p(\Delta x)\tilde{c}(x-\Delta x,w)d\Delta x,$$

$$\tilde{c}(x,0) = \delta(x-0). \qquad (5)$$

The function $\tilde{c}(x,w)$ is obtained from the inverse Fourier transform of $exp\{-w[1-\hat{p}(k)]\}$ where $\hat{p}(k)$ is the Fourier transform of $p(\Delta x)$. This analysis highlights the fact that $p(\Delta x)$ then captures all the physics associated with the Levy flight nature of ion beam mixing. For a thin foil, the energy loss of the incident beam can be neglected. This insures that $F_D(x)$ does not vary and the solution of Eq. (5) is no more than the Bothe Landau formula derived first by Sigmund *et al.* to describe ion beam mixing [7] in thin layers. However, Eq. (5) quantifies the distortion of the concentration profile due to ion beam mixing whatever the thickness of the target is.

As the tail of $p(\Delta x)$ is a power law for large $\frac{\Delta x}{L}$ values, $\hat{p}(k)$ presents a regular Taylor expansion in power of k up to $[q_c]$ the integer part of q_c and a term of the form k^{q_c} in the neighborhood of $k=0$ [30],

$$\hat{p}(k) = 1 + \sum_{j=1}^{[q_c]} \left(\frac{(-1)^j}{j!} \langle z^j \rangle \right) (ik)^j + r_{q_c} (ik)^{q_c}, \tag{6}$$

where $\langle z^j \rangle$ are the finite moments of $p(\Delta x)$ and $r_{q_c} \sim (-1)^{[q_c]+1} L^{q_c}$ is associated with the large tail of $p(\Delta x)$.

From this expansion of $\hat{p}(k)$ in the neighborhood of zero, it is possible to derive an asymptotic expansion for $c(x,t)$. By analogy with diffusion processes in complex media [27,31,32], this asymptotic expansion captures all the dynamics associated with the ion beam mixing. Different cases have to be considered:

(i) For $Z>33$, q_c is greater than 2 and the first two moments of $p(\Delta x)$ exist. The asymptotic concentration profile $c(x,t)$ is then equal to

$$c(x,t) = \left(\frac{2\pi \langle z^2 \rangle t\phi F_D(x)}{\mathcal{N}E_0} \right)^{-1/2} \exp\left(- \frac{\left(x - \frac{\langle z \rangle t\phi F_D(x)}{\mathcal{N}E_0} \right)^2}{\frac{2\langle z^2 \rangle t\phi F_D(x)}{\mathcal{N}E_0}} \right).$$

The function $c(x,t)$ exhibits a complex shape with a characteristic fluctuation scale proportional to $[t\phi F_D(x)]^{1/2}$. For thin targets, $F_D(x)$ is constant and $c(x,t)$ reduces to a Gaussian in agreement with the results of the "relocation cross section" theory [7,8]. The variance of the concentration profile is a linear function of $t\phi$ in agreement with experimental results [3,4]. The existence of the two first moments of $p(\Delta x)$ highlights that small Δx jumps dominate the dynamics of the ion beam mixing. The function $p(\Delta x)$ can be approximated by a Gaussian and does not exhibit a large tail. Equation (5) reduces to a Fokker Planck equation with a drift term $A(x) \sim \phi \frac{F_D(x)}{\mathcal{N}E_0}$ and a diffusion coefficient $D(x) \sim \phi \frac{F_D(x)}{\mathcal{N}E_0}$. The drift and the diffusion terms are obviously sensitive to the strength of the BZL interatomic potential since $\langle z \rangle$ and $\langle z^2 \rangle$ depend on $q_c(Z)$. The drift term breaks the left right symmetry of the diffusion equation and points out that atoms are displaced along the direction of the ion beam as expected.

(ii) For $4<Z<33$, $1<q_c<2$ and only the first moment of $p(\Delta x)$ exists. The asymptotic expansion of $c(x,t)$ is equal to:

$$c(x,t) = \left(\frac{C_{q_c} t\phi F_D(x)}{\mathcal{N}E_0} \right)^{-1/q_c} \mathcal{L}_{q_c,1} \left(\frac{x - \frac{\langle z \rangle \phi t F_D(x)}{\mathcal{N}E_0}}{\left(\frac{C_{q_c} t\phi F_D(x)}{\mathcal{N}E_0} \right)^{1/q_c}} \right)$$

$$\text{with} \quad C_{q_c} = -r_{q_c} \cos\left(\frac{q_c \pi}{2} \right) \tag{7}$$

where $\mathcal{L}_{q_c,1}$ is a Levy function [30,33] since C_{q_c} is always positive. The function $\mathcal{L}_{q_c,1}(u)$ is only defined for $u>0$ and exhibits a large tail proportional to $u^{-(1+q_c)}$. We show that the shape of the asymptotic expansion of $c(x,t)$ largely differs from a Gaussian for thin layers as pointed out first by Sigmund and Gras-Marti [7]. The characteristic fluctuation scale is now proportional to $[t\phi F_D(x)]^{1/q_c}$. Rare events become dominant and the dynamics of the ion beam mixing becomes a Levy flight. Large Δx values possess an algebraically small probability to occur but not exponentially small. The accumulation of large jumps Δx due to the physics of collision events then dominates the dynamics of the evolution of $c(x,t)$. The strength of the BZL interatomic potential remains sufficient to induce a drift of the concentration profile. Moreover, the long tail of the concentration profile is the signature of this Levy flight. The existence of such large tails have been reported by numerous authors [3,4,9] on different layers. In these different experiments performed at temperatures varying from 40 to 300 K, the mixing of low mass materials ($Z<18$) is fully controlled by pure ballistic processes without any influence of chemical driving forces [3,4]. Moreover, many Rutherford back scattering profiles of aluminum layers ($Z=13$) irradiated with 500 and 300 keV Xe ions at 40 K exhibit large tails [10,11] in agreement with our calculation. The migration of aluminum atoms cannot be evoked to explain this large tail since $k_BT=3.4\times10^{-3}$ eV is much lower than the vacancy migration enthalpy $H^m{}_v=0.65$ eV at this temperature [10].

(iii) For $Z<4$, $q_c<1$ and $p(\Delta x)$ does not possess any finite moment. the asymptotic expansion of $c(x,t)$ reduces to

$$c(x,t) = \left(\frac{C_{q_c} t\phi F_D(x)}{\mathcal{N}E_0} \right)^{-1/q_c} \mathcal{L}_{q_c,1} \left(\frac{x}{\left(\frac{C_{q_c} t\phi F_D(x)}{\mathcal{N}E_0} \right)^{1/q_c}} \right).$$

The concentration profile exhibits the same characteristic fluctuation scale than in the previous case. However, the strength of the BZL interatomic potential is no longer sufficient to induce a drift under irradiation.

Figure 3 displays the comparison between numerical solutions of Eq. (4) obtained using an implicit finite difference time scheme and its asymptotic expansion derived from Eq. (6). These plots display excellent agreement between numerical and analytical solutions over a large range of x values.

Whereas the power law form of the tail of $c(x,t)$ indicates the absence of a characteristic size for $Z<33$, it is possible to quantify the characteristic fluctuation length of particles after a time t under ion beam mixing according to

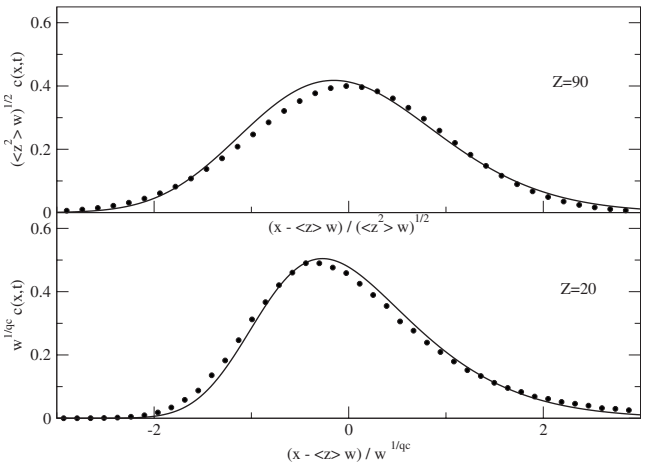

FIG. 3. Comparison between $c(x,t)$ calculated from Eq. (4) (full line) and its asymptotic expansion (dots) for $Z<33$ (top) and $Z<33$ (bottom). In both cases, the asymptotic expansions agree fairly well with numerical solutions over a large range of the reduced variables. The symmetric shape of the concentration profile for $Z>33$ is the signature of a Gaussian function whereas the asymmetric shape of the concentration profile for $Z<33$ is characteristic of a Levy function.

$$\langle |x(t) - x(0)| \rangle \sim (t\phi)^H, \tag{8}$$

where H is the Hurst exponent extensively used in diffusion processes [26,30–32]. For $Z>33$, collisions events generate only small Δx jumps and the distortion of the profile is low. The exponent reduces then to $\frac{1}{2}$ as expected from a classical diffusion process [26,30–32]. For $Z<33$, $p(\Delta x)$ exhibits a power law tail and large jumps occur giving rise to a Levy flight for the point set of displaced atoms [27,30,33]. From our analysis, the Hurst exponent is equal to $\frac{1}{q_c}$. From the analysis of experimental data [10], it is possible to follow the evolution of the broadening of aluminum profiles versus the fluence. This broadening measured on different samples does not exhibit a square root law variation as expected from a classical diffusion process [10,11]. Neglecting ballistic effects due to Xe ions, we have calculated the Hurst exponent in an aluminum layer. This exponent, equal to 0.65, agrees fairly well with the Hurst exponent $H=0.72\pm0.05$ extracted from experimental results [10]. For $Z<33$, it then seems that a strong enhancement of the diffusion process takes place. This enhancement is so important that a ballistic motion of atoms forming the concentration profile occurs for $Z=4$.

V. CONCLUSION

Using realistic cross sections, MC simulations were performed to estimate the evolution of concentration profiles under ion bean mixing within the binary collision approximation framework. The distortion of this profile is governed by the peculiar form of the transition probability $p(x,\Delta x)$. We demonstrate that this transition probability can be factorized into two separate contributions in agreement with MC simulations results. The first contribution is related to the energy lost by particles at a given position $F_D(x)$. The second contribution, $p(\Delta x)$, provides all information on the trajectory set of relocated atoms during the collision cascade. The tail of this function exhibits a power law form closely related to the peculiar shape of interatomic cross section associated with a collision event. The specific tail of $p(\Delta x)$ is such that the probability for large Δx values to occur is algebraically small but not exponentially small. Large Δx events then dominate the trajectory set of atoms set in motion by the incident beam. The migration of atoms under ion beam mixing then follows a Levy flight. As expected from the study of Levy flights [27,30], we demonstrated that the tail of the concentration profile possesses a power law form in agreement with experimental works [3,4] and that this unusual profile is associated with a strong enhancement of the diffusion for $Z<33$. This enhancement of diffusion identified here within the binary collision approximation cannot then be washed out during the displacement spike since the former atomic transport occurs on a scale length of several nanometers [7], thus larger than the characteristic length scale of atomic relocations in a displacement spike. Such an anomalous diffusion can then be invoked to explain the unusual diffusion of impurities in nanometric materials under irradiation [34]. Its impact on the calculation of the ballistic jump frequency, extensively used to study the patterning of solids under irradiation at the nanometric scale has also to be taken into account [12].

ACKNOWLEDGMENT

The authors acknowledge Y. Limoge and E. Bouchaud for many valuable discussions and continuous encouragements.

APPENDIX A: DERIVATION OF THE EXPONENTIAL LAW

We consider a particle with energy E going through a thin foil of length R. We suppose the stationarity of the cross section characterizing collision events between the incident beam and atoms in the medium. This foil can be divided into N slices of length Δr. This thickness Δr is chosen to create only one collision event in a slice. By definition of the cross section $\sigma(E)$, the probability for the incident particle to create a collision in Δr is then $p=\mathcal{N}\sigma(E)\Delta r$. Under these assumptions, the probability for the particle to generate k collisions in N slices is given by the binomial distribution $\mathcal{B}(N,k)$ for $k<N$. When Δr tends to zero, p tends to zero and N tends to infinity. However, the product Np remains constant and is equal to $\lambda=\mathcal{N}\sigma(E)R$. From the Poisson theorem [19], $\mathcal{B}(N,k)$ tends in law to the Poisson distribution $P(k)=e^{-\lambda}\frac{\lambda^k}{k!}$. The probability that no collision event occurs in the layer of thickness R is then equal to

$$P(0) = 1 - \sum_{k=1}^{\infty} e^{-\lambda}\frac{\lambda^k}{k!} = 1 - e^{-\lambda}(-1 + e^{\lambda}) = e^{-\mathcal{N}\sigma(E)R}.$$

From this analysis, the probability density for a particle of energy E to travel the distance l between two collisions, $p_C(l|E)$ is then equal to $\mathcal{N}\sigma(E)e^{-\mathcal{N}\sigma(E)l}$, thus recovering Eq. (1) from the text.

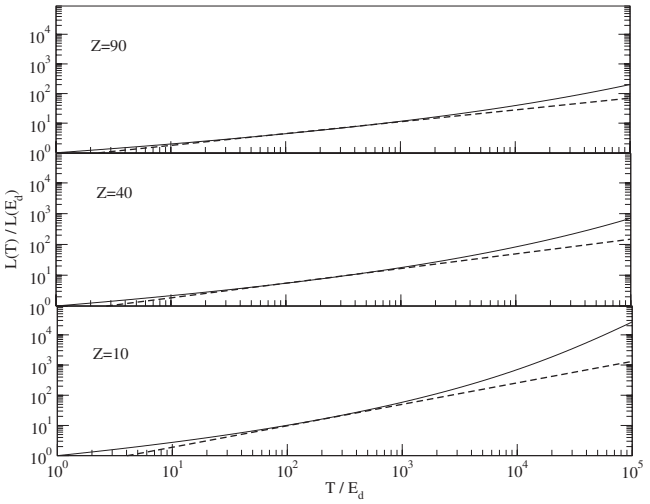

FIG. 4. Comparison between $L(T)$ calculated from the BZL interatomic potential (full line) and the power law approximation (dashed line) for different Z values over a large energy range. For low Z values, the approximation of $L(T)$ by a power law is crude. For middle and high Z values, the calculated and approximated curves agree fairly well.

APPENDIX B: CALCULATION OF $p(l)$

By analogy with the power law cross section, we assume that $L(T)$ can be approximated by a power law of T. The exponent of this power law only depends on the strength of the interatomic potential, i.e., Z. Figure 4 displays the comparison between $L(T)$ derived from BZL interatomic potential and its power law approximation for different Z values. For low Z values, the power law is a crude approximation of $L(T)$. However, this approximation becomes accurate over a large energy range for medium and high Z values. Replacing $L(T)$ by βT^{α} where α and β are positive values, $p(l|T)$ can be expressed as

$$\begin{aligned} p(l|T) &= \int_{E_d}^{T} h(T,U) p_C(l|U) dU \\ &= \int_{E_d}^{T} \frac{1}{U \ln\left(\frac{T}{E_d}\right)} p_C(l|U) dU \\ &= \frac{1}{\alpha \ln\left(\frac{T}{E_d}\right)} \int_{L(E_d)}^{L(T)} e^{-l/L} \frac{dL}{L^2} \\ &\sim \frac{1}{l}\left(-e^{-l/L(E_d)} + e^{-l/L(T)}\right) \end{aligned} \tag{B1}$$

For $l \gg L(E_d)$, this equation becomes:

$$p(l|T) \sim \frac{1}{l} e^{-l/L(T)} \tag{B2}$$

APPENDIX C: FRACTAL FEATURE OF TRAJECTORIES

Taking into account all trajectories of atoms in motion in a displacement cascade, the probability density associated with the length traveled by all atoms along all trajectories can be calculated using the following energy loss $h(T)=\frac{E_d}{T^2}$. Following the same analysis as in Appendix B, this density probability, $p_L(l)$ can be written as

$$p_L(l|T) = \frac{\alpha \Gamma(1+\alpha)}{l(1+\alpha)} L(T)^{-\alpha}. \tag{C1}$$

To assess the impact of the specific form of $p_L(l)$ for a defined value of T, we calculate the normalized moments $S(q,L)$ [35],

$$S(q,L) = \frac{\int_0^{+\infty} p_L(l) l^q dq}{\left(\int_0^{\infty} p_L(l) l dl\right)^q}, \tag{C2}$$

where q is a real number. For large L values, $S(q,L)$ is proportional to $L^{\tau(q)}$. The exponent $\tau(q)$ is equal to $-q(\alpha-1)$ for $q>\alpha$ and $\alpha(1-q)$ for $q<\alpha$. The power law form of $S(q,L)$ insures that the trajectory set exhibits a fractal behavior. For $q=\alpha$, $\frac{d\tau(q)}{dq}$ presents a singular point. For this reason, α appears as a critical point. We define this point as q_c in the text. The fractal dimension of the trajectories set $\tau(0)$ is equal to q_c as pointed out in the text. Figure 5 exhibits the variation in q_c extracted from MC simulations as a function of Z describing the strength of the BZL interatomic potential. The function $q_c(Z)$ can be approximated by $\frac{1}{2}\ln(\frac{Z}{0.6})$ over a large Z range.

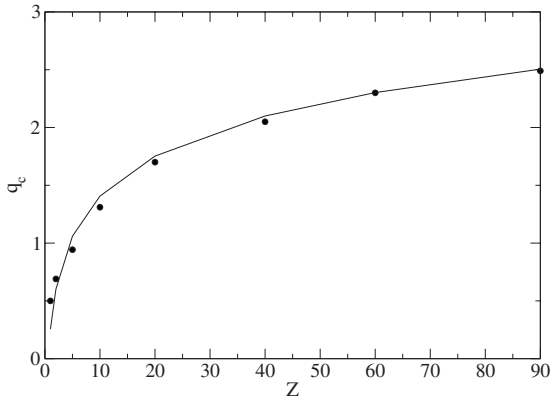

FIG. 5. Evolution of the q_c parameter as a function of Z (dots). The variation in q_c versus Z can be fitted by $\frac{1}{2}\ln(\frac{Z}{0.6})$ (full line) over a large Z range. The good value of the regression coefficient (0.999) insures the quality of this fit.

APPENDIX D: LARGE DEVIATION THEOREM

The random variable $z=\Sigma_{j=1}^{k} l_j$ is the sum of k identical independent random variables with the same probability density function $p(l|T)$. From the Large Deviation theorem, the probability for $z=kl$, $p_k(z=kl)$ can be estimated. This function is proportional to $e^{ks(l)}$ for large k values. The function $s(l)$ is the Cramer function [30]. From Eq. (B2), the characteristic function of $p(l|T)$, $Z(\beta)$ writes

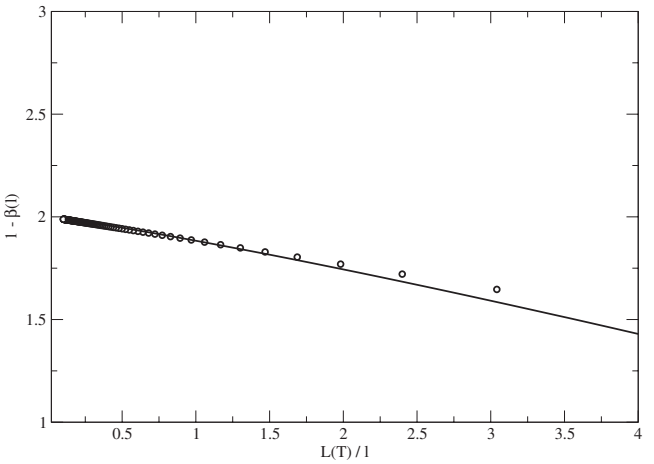

FIG. 6. Variation of $1-\beta$ derived from the numerical resolution of Eq. (D2) as a function of $\frac{L}{l}$ (dots). The experimental points form a straight line assessing the fit of $\beta(l)$ by an hyperbola with a regression coefficient equal to 0.999.

$$Z(\beta) \sim \ln\left(\frac{K+\beta}{1+\beta}\right), \tag{D1}$$

where $K=\frac{L(T)}{L(E_d)}$. To calculate $s(l)=\ln(Z(\beta))+\beta l$, the function $\beta(l)$ needs to be determined. The Large Deviation theorem gives an implicit relation to link β to l,

$$\frac{d\ln[Z(\beta)]}{d\beta} = -\frac{l}{L(T)} \tag{D2}$$

Figure 6 displays the variation in β as a function of l over a large l range. The function $\beta(l)$ can be approximated by an hyperbola $(-1+\frac{a_0}{l})$ where $a_0=\frac{(K-1)}{K\ln(K)}$ in this range. From this approximation, the Cramer function can be derived and $p_k(z=kl)$ is given by

$$P_k(z=kl) \sim e^{ka_0\ln(l/L(T))-k(l/L(T))}$$

$$P_k(z) \sim e^{-z/L(T)}\left(\frac{z}{kL(T)}\right)^{ka_0}. \tag{D3}$$

For $E_0 \gg E_d$, many collisions occur and the random variable k can be replaced by its mean value $\langle n\rangle = q_c \ln(K)$. This implies that ka_0 reduces then to q_c. The function $p_k(z)$ is now independent of k and can be approximated by a gamma law with a scale parameter $L(T)$ and a shape parameter $1+q_c$.

APPENDIX E: ASYMPTOTIC EXPANSION OF $p(\Delta x)$

Averaging over all trajectories, $p(\Delta x)$ can be written as

$$p(\Delta x) = \int_{E_d}^{E_0} \Gamma[\Delta x; 1+q_c, \hat{L}(T)]\frac{E_d}{T^2}dT. \tag{E1}$$

Replacing $\hat{L}(T)=L(T)/(1-\frac{S(E)}{2\sigma(E)E})$ by its approximation $\hat{\beta}T^{1/q_c}$, $p(\Delta x)$ then reduces to

$$p(\Delta x) = \frac{\beta^{q_c}q_cE_d}{(\Delta x)^{1+q_c}}\int_{\Delta x/E_0}^{\Delta x/E_d} e^{-u}u^{q_c}du \tag{E2}$$

For $L(E_d)<\Delta x<L(E_0)$, an asymptotic expression of Eq. (E2) can be derived

$$p(\Delta x) \sim \frac{\beta^{q_c}q_cE_d}{(\Delta x)^{1+q_c}}\int_0^{\infty} e^{-u}u^{q_c}du \sim \frac{\beta^{q_c}q_cE_d}{(\Delta x)^{1+q_c}\Gamma(1+q_c)}. \tag{E3}$$

The probability density $p(\Delta x)$ follows a power law $\frac{1}{\Delta x^{1+q_c}}$ for large Δx values. The parameter q_c characterizes the fractal feature of trajectories. The strength of the BZL interatomic potential associated with the description of collision events appears in the Z dependence of q_c.

[1] G. Martin and P. Bellon, Solid State Phys. **53-54**, 1 (1997).
[2] H. Bernas, J. P. Attane, K. H. Heinig, D. Halley, D. Ravelosona, A. Marty, P. Auric, C. Chappert, and Y. Samson, Phys. Rev. Lett. **91**, 077203 (2003).
[3] Y. Cheng, Mater. Sci. Rep. **5**, 45 (1990).
[4] W. Bolse, Mater. Sci. Eng. R. **12**, 53 (1994).
[5] R. Averback and T. D. de la Rubbia, Solid State Phys. **51**, 281 (1997).
[6] R. Smith, M. Jakas, D. Ashworth, B. Oven, and M. Bowyer, *Atomic and Ion Collisions in Solids and at Surfaces: Theory, Simulation and Applications* (Cambridge University Press, Cambridge, England, 1997).
[7] P. Sigmund and A. Gras-Marti, Nucl. Instrum. Methods **168**, 389 (1980).
[8] P. Sigmund and A. Gras-Marti, Nucl. Instrum. Methods **182-183**, 25 (1981).
[9] T. Kacsich, Th. Weber, W. Bolse, and K. Lieb, Appl. Phys. A: Mater. Sci. Process. **57**, 187 (1993).
[10] F. Besenbacher, J. Bøttiger, S. Nielsen, and H. Whitlow, Appl. Phys. A: Mater. Sci. Process. **29**, 141 (1982).
[11] Z. L. Wang, J. F. M. Westendorp, and F. W. Saris, Nucl. Instrum. Methods **209-210**, 115 (1983).
[12] R. A. Enrique and P. Bellon, Phys. Rev. Lett. **84**, 2885 (2000).
[13] P. Krasnochtchekov, R. S. Averback, and P. Bellon, Phys. Rev. B **75**, 144107 (2007).
[14] K. Sickafus, R. Grimes, J. Valdez, M. Ishimaru, J. M. F. Li, and T. Hartmann, Science **289**, 748 (2000).
[15] U. Littmark and J. F. Ziegler, Phys. Rev. A **23**, 64 (1981).
[16] L. Lindhard, M. Schraff, and H. Schiott, Mat. Fys. Medd. K. Dan. Vidensk. Selsk. **33**, 1 (1963).
[17] L. Lindhard, V. Nielsen, and M. Schraff, Mat. Fys. Medd. K. Dan. Vidensk. Selsk. **36**, 1 (1968).
[18] P. Sigmund, Rev. Roum. Phys. **17**, 1079 (1972).
[19] W. Feller, *An Introduction to Probability Theory and its Applications* (Wiley, New York, 1966).
[20] J. Ziegler, J. Biersack, and M. Ziegler, *SRIM, The Stopping*

and Range of Ions in Matter (Lulu Press, Morrisville, 1985).
[21] F. Kun and G. Bardos, Phys. Rev. E **55**, 1508 (1997).
[22] Y. Rubinstein and V. Krocse, *Simulation and the Monte Carlo Method* (Wiley, Chichester, 2008).
[23] G. Amsel, G. Basttistig, and A. L'Hoir, Nucl. Instrum. Methods Phys. Res. B **201**, 325 (2003).
[24] P. Sigmund, *Particle Penertation and Radiation Effects* (Springer, New York, 2005).
[25] D. Brice, J. Appl. Phys. **46**, 3385 (1975).
[26] J. Feder, *Fractals* (Plenum, New York, 1988).
[27] M. Shlesinger, G. Zaslavsky, and J. Klafter, Nature (London) **363**, 31 (1993).
[28] D. Simeone, L. Luneville, and J. Both, Europhys. Lett. **83**, 56002 (2008).
[29] J. Lindhard and V. Nielsen, Mat. Fys. Medd. K. Dan. Vidensk. Selsk. **38**, 1 (1971).
[30] D. Sornette, *Critical Phenomena in Natural Sciences* (Springer, New York, 2003).
[31] P. Grassberger, Phys. Lett. A **97**, 227 (1983).
[32] C. Amitrano, A. Coniglio, and F. di Liberto, Phys. Rev. Lett. **57**, 1016 (1986).
[33] J. P. Bouchaud, E. Bouchaud, G. Lapasset, and J. Planes, Phys. Rev. Lett. **71**, 2240 (1993).
[34] A. Meldrum, L. A. Boatner, and R. C. Ewing, Phys. Rev. Lett. **88**, 025503 (2001).
[35] T. C. Halsey, M. H. Jensen, L. P. Kadanoff, I. Procaccia, and B. I. Shraiman, Phys. Rev. A **33**, 1141 (1986).